State-Space Model of qZSI based PMSG-WPGSs for Transient Dynamic Studies

2021 IEEE International Conference on Environment and Electrical Engineering and 2021 IEEE Industrial and Commercial Power Systems Europe (EEEIC / I&CPS Europe) | 978-1-6654-3613-7/21/$31.00 ©2021 IEEE | DOI: 10.1109/EEEIC/ICPSEurope51590.2021.9584824

Lluís Monjo
Department of Engineering Systems and Design
Universitat Jaume I
Castelló de la Plana, Spain
lmonjo@uji.es

Luis Sainz
Department of Electrical Engineering
Universitat Politecnica de Catalunya
Barcelona, Spain
luis.sainz@upc.edu

***Abstract*—The use of permanent magnet synchronous generators (PMSGs) with full-scale back-to-back converters is rising as a common option in wind power generation systems (WPGSs). An efficient grid integration of PMSG-WPGSs is obtained through quasi-Z-source inverter (qZSI). Simultaneously, power electronic system integration concerns related to dynamics have arisen. Power electronics reduce damping of grid-connected converters, leading to dynamic issues. Several studies focus on qZSI dynamics, but the analysis of qZSI based PMSG-WPGS dynamics to evaluate transient interactions is not yet well addressed. This paper studies a qZSI based PMSG-WPGSs small-signal state-space model for Matlab/Simulink implementation in order to study these concerns. The model is applied to investigate qZSI based PMSG-WPGS dynamic response and it allows the influence of components and parameters on system dynamics to be assessed. Eigenvalues are obtained from the state-space model in order to study qZSI based PMSG-WPGS stability and the participation factors are also analyzed to find out the most influential circuit component or control on the different eigenvalues. PSCAD/EMTDC simulations are made to test the model.**

Keywords—Wind power systems, quasi-Z-source inverter, stability.

I. INTRODUCTION

Permanent magnet synchronous generator (PMSG) based wind power generation systems (WPGSs) are one of the mainstream renewable systems [1] – [4]. The well-known two-step DC/DC boost converter with DC/AC voltage source inverter (VSI) topology is the usual arrangement in PMSG-WPGSs [5], [6]. However, this configuration is not cost effective and its control is awkward. Single-stage topologies with Z-source inverters have recently been reported as a straightforward and low-cost technology [2], [5] – [12]. It is worth noting the engineering comprehensive review of them (main topologies, models, controls) in [10], [11] as well as their complete comparison related to their passive components and semiconductor stress in [12]. These inverters offer several advantages such as fixing buck/boost DC voltage in a single step with reliability and efficiency. Quasi-Z-source inverters (qZSIs) are increasingly gaining importance [2], [13] – [19]. Apart from Z-source inverter benefits, qZSIs provide continuous DC input current and reduced DC switching ripple and passive component stress, hence the increasing importance of qZSI based PMSG-WPGSs [15] – [17]. A new qZSI topology called as three-level neutral-point-clamped qZSI is examined in [18], [19]. It provides the benefits of the the qZSI and the three-level neutral-point-clamped inverter topologies.

Power electronic system integration in traditional grids such as wind energy conversion system integration usually causes dynamic problems (e.g., instabilities) due to the damping of grid-connected converters caused by power electronics. To prevent these issues, it will be necessary to analize the dynamic behavior of wind energy conversion systems such as qZSI based PMSG-WPGSs. Several works address the dynamic response of PMSG-WPGSs implemented with the conventional two-step DC/DC boost-converter and DC/AC VSI, whereas very few deal with qZSI based PMSG-WPGS dynamic assessment. Most of these only focus on the qZSI dynamic model [2], [13] – [15]. The dynamic response of the complete qZSI based PMSG-WPGS is examined in [16] from a proposed block diagram model, but the model is not detailed enough. A hardware prototype of the system is also developed and tested in the laboratory. In [17], a new qZSI based PMSG-WPGS with a battery storage system is presented. A comparative work between qZSI controls is performed by means of the state-space model of qZSIs in [20]. Moreover, different papers study stability in qZSI-based PV power systems [21] - [25].

This paper contributes with a qZSI based PMSG-WPGS Matlab/Simulink state-space model. This model is obtained considering all the main controls and used to study the dynamic response of the qZSI based PMSG-WPGS. The model and the obtained results are validated with PSCAD/EMTDC simulations.

II. QZSI BASED PMSG-WPGSS

The PSCAD/EMTDC circuit of qZSI based PMSG-WPGSs is shown in Fig. 1. It has a PMSG connected to the VSI dc-side by means of the qZSI. The classical tracking of the maximum power point (MPP), i.e., the classical MPPT, allows the maximum power to be harvested from the PMSG, and the WPGS controls guarantee that power comes from the PMSG and is delivered to the AC network. The DC-link voltage is fixed by the duty cycle control.

III. QZSI BASED PMSG-WPGS SIMULINK MODELING

The qZSI based PMSG-WPGS small-signal state-space model for Matlab/Simulink implementation and transient dynamic simulation is presented in Fig. 2. This model also makes it possible to determine the state-space matrix **A** of the system, its eigenvalues $\lambda_i = \sigma_i \pm j \cdot \omega_i$ and their participation factors $p_{ki} = \phi_{ki} \cdot \psi_{ik}$ obtained from the right ϕ_{ki} and the left ψ_{ik} eigenvectors of **A**.

This work was economically supported from the Ministerio de Ciencia, Innovación y Universidades under Grant RTI2018-095720-B-C33.

978-1-6654-3613-7/21/$31.00 ©2021 IEEE

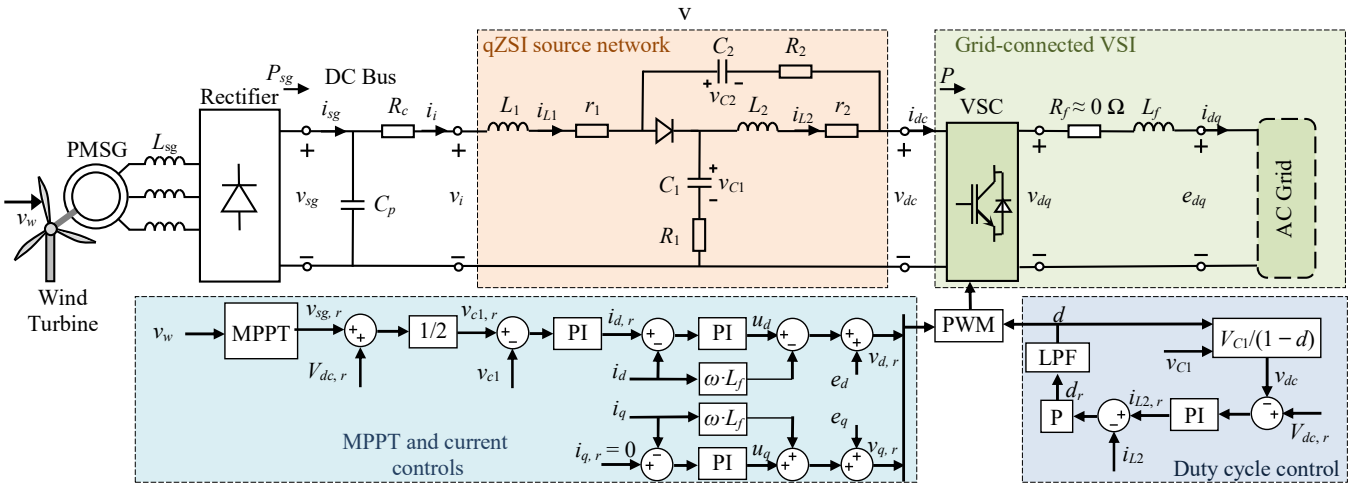

Fig. 1. PSCAD/EMTDC circuit of qZSI based PMSG-WPGSs.

A. Wind turbine, PMSG and MPPT control model

The rotor blades deliver the maximum power P_{mpp} to the PMSG according to the wind speed v_w by regulating the PMSG rectifier output voltage v_{sg} through the MPPT control. This control fixes the PMSG rectifier output voltage, $v_{sg,\,r}$, by imposing the maximum power P_{mpp}.

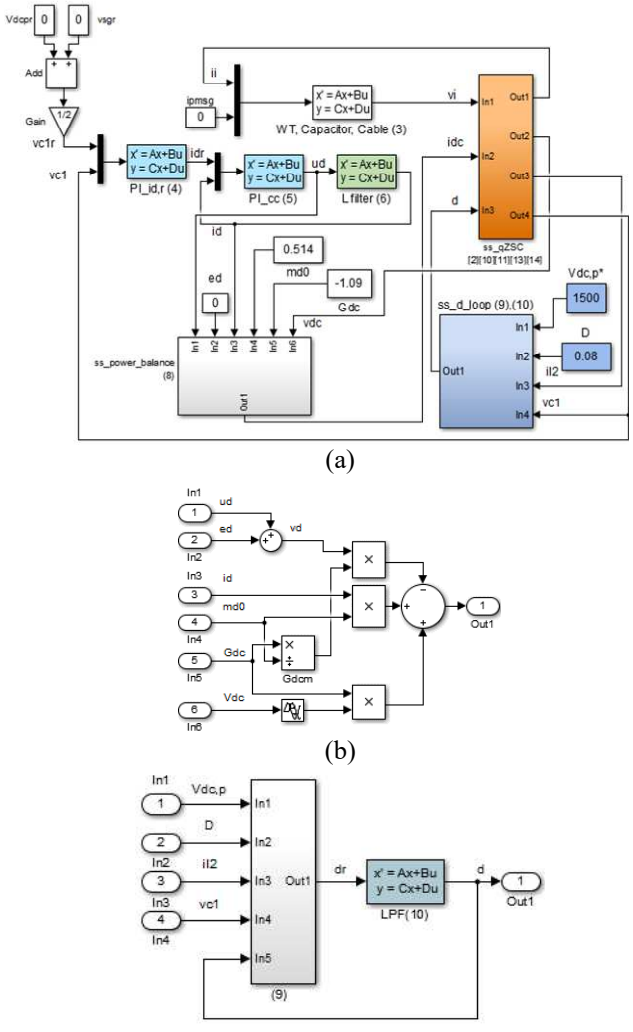

Fig. 2. qZSI based PMSG-WPGS small-signal state-space model implementation in Simulink. a) Overall layout. b) Power balance subsystem. c) Duty cycle control subsystem.

The PMSG with the front-end rectifier is considered as a fixed power station at the MPP to obtain its small-signal model, Fig. 3, that is,

$$i_{sg} = \frac{P_{sg}}{v_{sg}} \quad \Rightarrow \quad \Delta I_{sg} = \Delta i_{pmsg} - R_{sg}\Delta v_{sg}, \tag{1}$$

where

$$\Delta I_{pmsg} = \frac{\Delta P_{sg}}{V_{sg,\,r}} \qquad R_{sg} = \frac{P_{mpp}}{V_{sg,\,r}^2}, \tag{2}$$

where $V_{sg,\,r}$ is the steady state value of the PMSG rectifier output voltage at the MPP.

Finally, the model of the PMSG with the front-end rectifier, shunt capacitor C_p and cable R_c becomes (see Fig. 3)

$$\begin{aligned} \frac{d}{dt}\left[\Delta v_{sg}\right] &= \begin{bmatrix} \frac{-1}{C_p R_{sg}} \end{bmatrix}\left[\Delta v_{sg}\right] + \begin{bmatrix} \frac{-1}{C_p} & \frac{1}{C_p} \end{bmatrix}\begin{bmatrix} \Delta i_i \\ \Delta i_{pmsg} \end{bmatrix} \\ \left[\Delta v_i\right] &= [1]\left[\Delta v_{sg}\right] + [-R_c \quad 0]\begin{bmatrix} \Delta i_i \\ \Delta i_{pmsg} \end{bmatrix}. \end{aligned} \tag{3}$$

The PMSG speed characterizes the maximum power harvested by the blades of the wind turbine and is regulated adjusting the PMSG rectifier output voltage $v_{sg,\,r}$ through the MPPT control. This MPPT control is well documented in [5], [17], and is not described here for space reasons.

B. AC-output voltage control and grid-connected VSI model

The AC grid d-reference current $i_{d,\,r}$ is calculated by the capacitor-C_1 voltage PI control by deriving it from the DC PMSG rectifier voltage $v_{sg,\,r}$ and the DC-link voltage reference $V_{dc,\,r}$ as $v_{c1,\,r} = (v_{sg,\,r} + V_{dc,\,r})/2$, Fig. 1, [2]. Thus, the equation of this control is expressed as

$$\begin{aligned} \frac{d}{dt}\left[\Delta q_{c1}\right] &= [0]\left[\Delta q_{c1}\right] + [1 \quad -1]\begin{bmatrix} \Delta v_{c1} \\ \Delta v_{c1,r} \end{bmatrix} \\ \left[\Delta i_{d,r}\right] &= \left[k_i^{c1}\right]\left[\Delta q_{c1}\right] + \left[k_p^{c1} \quad -k_p^{c1}\right]\begin{bmatrix} \Delta v_{c1} \\ \Delta v_{c1,r} \end{bmatrix}, \end{aligned} \tag{4}$$

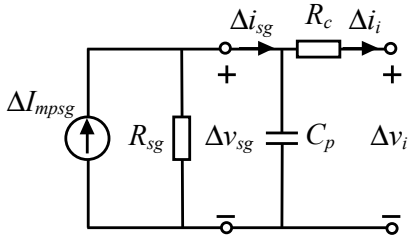

Fig. 3. Small-signal circuit of the PMSG with the front-end rectifier, shunt capacitor and cable.

where $k^{c1}{}_p$ and $k^{c1}{}_i$ are the capacitor-C_1 voltage control PI gains. The q-reference current $i_{q,r}$ is fixed to zero by assuming unity power factor of the VSI.

The AC grid d-reference voltage u_d is obtained from the PI control of the dq-frame VSC current, and its small-signal state-space model is written as

$$\begin{aligned}\frac{d}{dt}[\Delta q_{cc}] &= [0][\Delta q_{cc}] + \begin{bmatrix}1 & -1\end{bmatrix}\begin{bmatrix}\Delta i_{d,r}\\ \Delta i_d\end{bmatrix}\\ [\Delta u_d] &= \begin{bmatrix}k_i^{cc}\end{bmatrix}[\Delta q_{cc}] + \begin{bmatrix}k_p^{cc} & -k_p^{cc}\end{bmatrix}\begin{bmatrix}\Delta i_{d,r}\\ \Delta i_d\end{bmatrix},\end{aligned} \tag{5}$$

where $k^{cc}{}_p$ and $k^{cc}{}_i$ are the gains of the PI control.

Finally, the model of the grid-connected VSI can be expressed as

$$\begin{aligned}\frac{d}{dt}[\Delta i_d] &= [0][\Delta i_d] + \begin{bmatrix}\frac{1}{L_f}\end{bmatrix}[\Delta u_d]\\ [\Delta i_d] &= [1][\Delta i_d] + [0][\Delta u_d],\end{aligned} \tag{6}$$

where L_f corresponds to the converter filter inductance.

C. qZSI model

Deduction of the qZSI model in Fig. 1 is presented in the following lines.

The small-signal state-space averaged model of the qZSI power circuit model is well documented in [2], [13], [14], [16], [17]. This model relates the state vector $\mathbf{x_z} = [\Delta i_{L1}\ \Delta i_{L2}\ \Delta v_{C1}\ \Delta v_{C2}]^{\mathrm{T}}$ with the inductor currents and capacitor voltages to the input $\mathbf{u} = [\Delta v_i\ \Delta i_{dc}\ \Delta d]^{\mathrm{T}}$ and output $\mathbf{y} = [\Delta i_i\ \Delta v_{dc}]^{\mathrm{T}}$ vectors with the qZSI input and output currents i_{dc} and i_i, voltages v_i and v_{dc}, and finally the duty cycle d.

The dc-side qZSI current i_{dc} is calculated from the DC/AC VSI power balance which, by considering an ideal VSI, can be written as

$$v_{dc} i_{dc} = v_d i_d + v_q i_q. \tag{7}$$

This equation can be written as the below small-signal relation:

$$\begin{aligned}&V_{dc}\Delta i_{dc} + I_{dc}\Delta v_{dc} = V_d \Delta i_d + I_d \Delta v_d + V_q \Delta i_q + I_q \Delta v_q\\ &\underset{V_d >> V_q}{\overset{E_q = I_q = 0}{\Longrightarrow}} \quad \Delta i_{dc} = m_{d0}\Delta i_d - \frac{1}{m_{d0}} G_{dc}\Delta v_d + G_{dc}\Delta v_{dc},\end{aligned} \tag{8}$$

where $m_{d0} = V_d / V_{dc}$ is the steady state operating point of the modulation function, $G_{dc} = 1/R_{dc} = -P/V^2{}_{dc}$, P is the power from the DC to the AC side (see Fig. 1), V_d is the steady state converter voltage and I_{dc} and V_{dc} are the steady state qZSI output current and voltage, respectively.

The small-signal state-space model of the duty cycle d_r in Fig. 1 is

$$\begin{aligned}&\frac{d}{dt}[\Delta q_{dc}] = [0][\Delta q_{dc}] + \begin{bmatrix}0 & \frac{1}{1-D} & \frac{V_{dc,p}}{1-D}\end{bmatrix}\begin{bmatrix}\Delta i_{L2}\\ \Delta v_{C1}\\ \Delta d\end{bmatrix}\\ &[\Delta d_r] =\\ &\begin{bmatrix}-k_p^L k_i^{dc}\end{bmatrix}[\Delta q_{dc}] + \begin{bmatrix}-k_p^L & -\frac{k_p^L k_p^{dc}}{1-D} & -\frac{k_p^L k_p^{dc}}{1-D} V_{dc,p}\end{bmatrix}\begin{bmatrix}\Delta i_{L2}\\ \Delta v_{C1}\\ \Delta d\end{bmatrix},\end{aligned} \tag{9}$$

where $k^{dc}{}_p$ and $k^{dc}{}_i$ are the gains of the PI DC-link voltage control, $k^L{}_p$ is the gain of the P inductor-L_2 current control and D is the steady-state duty cycle.

Finally, the LPF small-signal state-space model can be expressed as

$$\begin{aligned}\frac{d}{dt}[\Delta d] &= [-\omega_c][\Delta d] + [\omega_c][\Delta d_r]\\ [\Delta d] &= [1][\Delta d] + [0][\Delta d_r].\end{aligned} \tag{10}$$

D. Model validation

The qZSI based PMSG-WPGS model with the data in Table I is validated in Fig. 4. The wind generator feeds a 2 MW 1.27 kV DC qZSI based PMSG-WPGS linked to a strong AC grid with 690 V line-to-line rms voltage, and operates with a wind speed $v_w = 12$ m/s. The qZSI works with a duty cycle $D = 0.16$.

The grid d-current i_d and the DC-link voltage v_{dc} dynamic response are studied when the grid d-voltage e_d is varied 1% and 0.5% around the AC grid nominal voltage (see top of Fig. 4). The fair accuracy of the qZSI based PMSG-WPGS model is validated from the complete system in Fig. 1 by comparing its dynamic response to the simulations obtained with PSCAD/EMTDC.

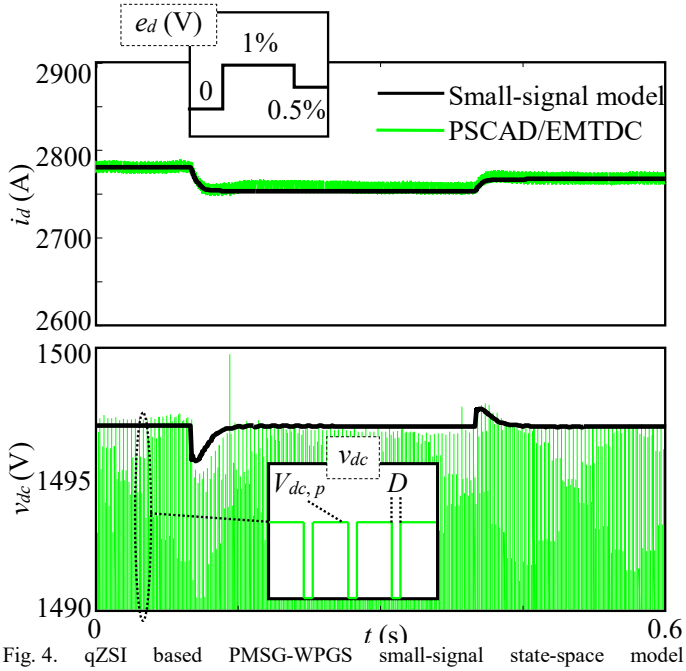

Fig. 4. qZSI based PMSG-WPGS small-signal state-space model PSCAD/EMTDC validation.

Table 1	2 MW 1.5 KV DC QZSI BASED PMSG-WPGS DATA			
	Parameter		*Data*	
Cable and input C filter	R_c,	C_p	≈ 0 Ω	10 MF
qZSI	$L_1 = L_2$	$r_1 = r_2$	4 MH	0.005 Ω
	$C_1 = C_2$	$R_1 = R_2$	1 MF	0.05 Ω
AC Filter	R_f	L_f	≈ 0 Ω	10 MH
Cap-C_1 control	$k^{c1}{}_p$	$k^{c1}{}_i$	5.3 Ω^{-1}	125 Ω^{-1}/S
Current control	$k^{cc}{}_p$	$k^{cc}{}_i$	3.2 Ω^{-1}	97 Ω^{-1}/S
D control	$V^*{}_{dc,p}$		1500 V	
	$k^{dc}{}_p$	$k^{dc}{}_i$	10 V^{-1}	125 V^{-1}/S
	$k^L{}_p$		16.67^{-4} A^{-1}	

IV. Application

In this Section, PSCAD/EMTDC simulations are used to analyze the proposed qZSI based PMSG-WPGS model (Fig. 1) to show the contributions of the paper. Three different operating points related to wind speed are studied, v_w = 9.5, 7.75 and 12 m/s (see Fig. 5(a)), with the DC-link voltage peak set to $V_{dc,r}$ = 1500 V by the duty cycle control. The application data are in Table I.

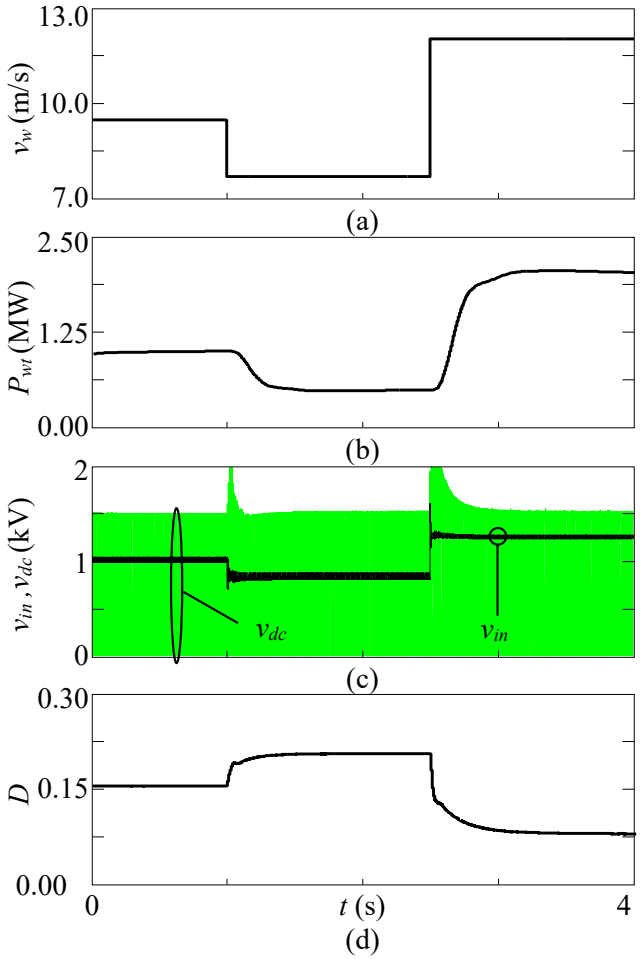

Fig. 5. PSCAD/EMTDC transient dynamic study. a) Wind speed. B) Wind turbine active power. c) DC voltages. d) Duty cycle.

It is observed that the wind turbine output power tracks the MPP according to the wind speed variations (see Fig. 5(b)). These variations also modify the PMSG rectifier output voltage (see v_{in} in Fig. 5(c)), and the duty cycle d is accordingly changed by the duty cycle control (see Fig. 5(d)) to hold the DC-link voltage at 1500 V. It is also worth noting that the qZSI based PMSG-WPGS is stable regardless the operation point.

Small-signal system stability around the above steady state operating points is studied from the model in Section II (Fig. 2). The eigenvalues $\lambda_i = \sigma_i \pm j \cdot \omega_i$ are obtained from the state-space model, and the variables σ_i and $\omega_i/(2\pi)$ are shown in Fig. 6 for the 2 MW operating point. These eigenvalues verify system stability because they are not in the right-half plane (RHP). In order to analyze qZSI based PMSG-WPGS stability, the participation factors $p_{ki} = \phi_{ki} \cdot \psi_{ik}$ are calculated from the right ϕ_{ki} and left ψ_{ik} eigenvectors where k and i represent the state-space variables and the modes, respectively. According to this, Fig. 6 shows the participation factors of the eigenvalues associated to the seven modes closest to the RHP. The results help to find out

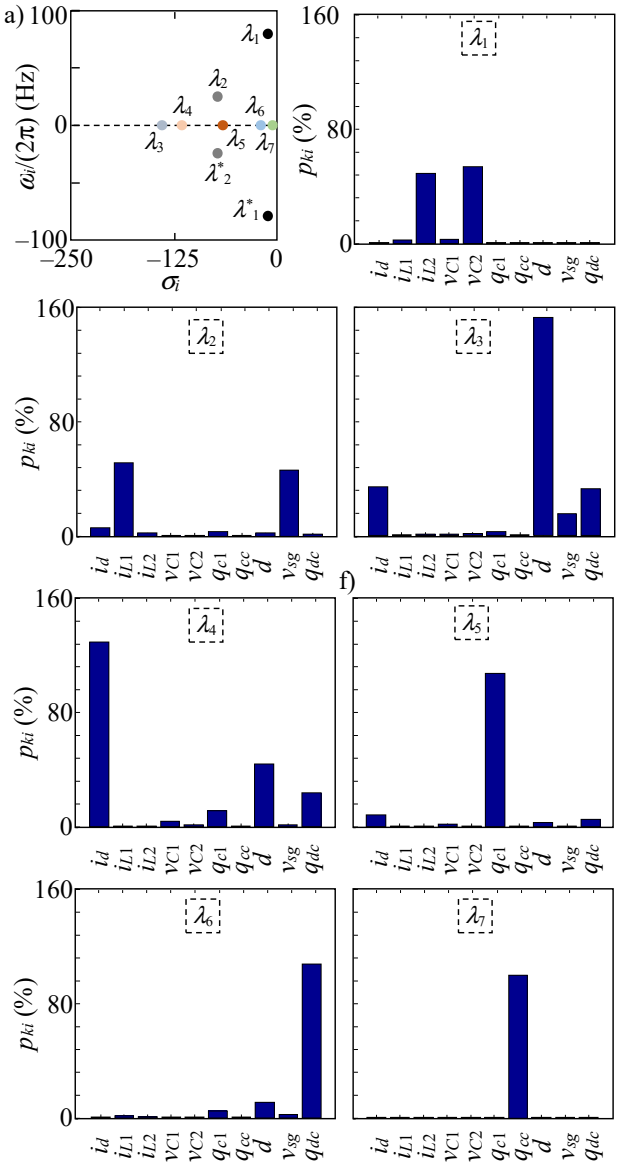

Fig. 6. Stability study.

the most influential circuit component or control on the different eigenvalues. As examples, we have

- Eigenvalue λ_1: the qZSI inductor L_2 and capacitor C_2 have the largest participation factors for this mode, suggesting that qZSI based PMSG-WPGS stability can be enhanced by adapting the above qZSI parameters.
- Eigenvalue λ_5: the state variable q_{c1} has the largest participation factor for this mode, suggesting that qZSI based PMSG-WPGS stability can be obtained by adjusting the gains of the capacitor-C_1 voltage PI control ($k^{c1}{}_p$ and $k^{c1}{}_i$).
- Eigenvalue λ_7: the state variable q_{cc} has the largest participation factor for this mode, suggesting that qZSI based PMSG-WPGS stability can be obtained by adjusting the gains of the AC grid *d*-reference voltage PI control ($k^{cc}{}_p$ and $k^{cc}{}_i$).

V. Conclusions

This paper presents a qZSI based PMSG-WPGSs small-signal state-space model for Matlab/Simulink implementation considering all the main components and controls. The model allows the influence of components and parameters on system dynamics to be assessed. PSCAD/EMTDC was used to validate the above contributions. The following further studies could be performed from the present study: (i) analysis of approximations of the proposed small-signal state-space model to characterize system dynamics analytically, and (ii) development of a frequency-based model of the qZSI based PMSG-WPGS for stability studies.

References

[1] M. Young, The Technical Writer's Handbook. Mill Valley, CA: University Science, 1989. T. Ackermann, Wind Power in Power Systems, Wiley & Sons Ltd, 2012.

[2] Y. Liu, H. Abu-Rub, B. Ge, F. Blaabjerg, O. Ellaban, P. Chiang "Impedance source power electronic converters", Chichester, West Sussex, UK: John Wiley and Sons, IEEE Press 2016.

[3] F. Blaabjerg, M. Ke, "Future on power electronics for wind turbine systems," IEEE Journal of Emerging and Selected Topics in Power Electronics, vol.1, no.3, pp.139–152, Sept. 2013.

[4] C. Zhe, J. M. Guerrero, F. Blaabjerg, "A review of the state of the art of power electronics for wind turbines," IEEE Trans. Power Electron., vol.24, no.8, pp.1859–1875, Aug. 2009.

[5] S. M. Dehghan, M. Mohamadian, A. Y. Varjani, "A new variable-speed wind energy conversion system using permanent-magnet synchronous generator and Z-source inverter," IEEE Trans. Energy Convers., vol.24, no.3, pp.714–724, Sept. 2009.

[6] W.-T. Franke, M. Mohr, F. W. Fuchs, "Comparison of a Z-source inverter and a voltage-source inverter linked with a DC/DC-boost-converter for wind turbines concerning their efficiency and installed semiconductor power," in Proc. IEEE Power Electronics Specialists Conference (PESC), pp.1814–1820, 2008.

[7] U. Supatti, F. Z. Peng, "Z-source inverter with grid connected for wind power system," in Proc. IEEE Energy Conversion Congress and Exposition (ECCE), pp. 398–403, 2009.

[8] B. K. Ramasamy, A. Palaniappan, S. M. Yakoh, "Direct-drive low-speed wind energy conversion system incorporating axial-type permanent magnet generator and Z-source inverter with sensorless maximum power point tracking controller," IET Renew. Power Gen., vol.7, no.3, pp.284–295, May 2013.

[9] X. Wang, D. M. Vilathgamuwa, K. J. Tseng, C. J. Gajanayake, "Controller design for variable-speed permanent magnet wind turbine generators interfaced with Z-source inverter," in Proc. 2009 International Conference on Power Electronics and Drive Systems (PEDS), pp.752–757, 2009.

[10] Y. P Siwakoti, F. Z. Peng, F. Blaabjerg, P. C. Loh, G. E. Town, "Impedance-Source Networks for Electric Power Conversion Part I: A Topological Review", IEEE Transactions on Power Electronics, vol. 30, no. 2, Feb. 2015, pp. 699-716.

[11] Y. P Siwakoti, F. Z. Peng, F. Blaabjerg, P. C. Loh, G. E. Town, Impedance-Source Networks for Electric Power Conversion Part II: "Review of Control and Modulation Techniques", IEEE Transactions on Power Electronics, vol. 30, no. 4, 2015**,** pp. 1887-1906

[12] O. Husev, F. Blaabjerg, C. Roncero-Clemente, E. Romero-Cadaval, D. Vinnikov, Y. Siwatoki, R. Strzelecki, "Comparison of Impedance-Source Networks for Two and Multilevel Buck–Boost Inverter Applications", IEEE Transactions on Power Electronics, vol. 31, no. 11, 2016, pp. 7564-7579.

[13] J. Liu, J. Hu, L. Xu, "Dynamic modeling and analysis of Z-source converter-derivation of AC small signal model and design-oriented analysis," IEEE Trans. Power Electron., vol. 22, no.5, pp.1786–1796, Sept. 2007.

[14] Y. Liu, B. Ge, F. J. T. E. Ferreira, A. T. de Almeida, H. Abu-Rub, "Modeling and SVPWM control of quasi-Z-source inverter," in Proc. 11th International Conference on Electrical Power Quality and Utilisation (EPQU), Lisbon, Portugal, pp. 1–7, 2011.

[15] Y. Liu, B. Ge, F. Z. Peng, H. Abu-Rub, A. T. De Almeida, F. J. T. E. Ferreira, "Quasi-Z-source inverter based PMSG wind power generation system," in Proc. IEEE Energy Conversion Congress and Exposition (ECCE), pp.291–297, 2011.

[16] T. Maity, H. Prasad, V. R. Babu, "Study of the suitability of recently proposed quasi-Z-source inverter for wind power conversion," in Proc. International Conference on Renewable Energy Research and Application (ICRERA), pp.837–841, 2014.

[17] M. M. Bajestan, H. Madadi, M. A. Shamsinejad, "Control of a new stand-alone wind turbine-based variable speed permanent magnet synchronous generator using quasi-Z-source inverter," Electric Power Systems Research, vol.177, available online, Aug. 2019.

[18] C. Roncero-Clemente, E. Romero-Cadaval, O. Husev, D. Vinnikov, S. Stepenko, "Simulation of Grid Connected Three-Level Neutral-Point-Clamped qZS Inverter using PSCAD" Electrical, Control and Communication Engineering*,* 2*,* 2013**,** 14-20. 10.2478/ecce-2013-0002.

[19] O. Husev, E. Roncero-Clemente, S. Stepenko, D. Vinnikov, E-Romero-Cadaval., "CCM operation analysis of the single-phase three-level quasi-Z-source inverter", 2012 15th International Power Electronics and Motion Control Conference (EPE/PEMC), Novi Sad, 2012, pp. DS1b.21-1-DS1b.21-6.

[20] V. Castiglia, R. Miceli, F. Blaabjerg, Y. Yang, "Small-Signal Modeling and Experimental Validation of the Three-phase Quasi-Z-Source Inverter", 2020 IEEE 21st Workshop on Control and Modeling for Power Electronics (COMPEL), Aalborg, Denmark, 2020, pp. 1-8.

[21] S. Stepenko, O. Husev, D. Vinnikov, C. Roncero-Clemente, S. Pires Pimentel, E. Santasheva, "Experimental Comparison of Two-Level Full-SiC and Three-Level Si–SiC Quasi-Z-Source Inverters for PV Applications". Energies, 2019, 12, 2509.

[22] Z. Liang, S. Hu, H. Yang, X. He, "Synthesis and Design of the AC Current Controller and Impedance Network for the Quasi-Z-Source Converter", IEEE Transactions on Industrial Electronics, vol. 65, no. 10, 2018, pp. 8287-8296.

[23] W. Liu, Y. Yang, T. Kerekes, E. Liivik, F. Blaabjerg, "Impedance Network Impact on the Controller Design of the QZSI for PV Applications", 2020 IEEE 21st Workshop on Control and Modeling for Power Electronics (COMPEL), Aalborg, Denmark, 2020, pp. 1-6

[24] L. Oliveira-Assis, E. P. P. Soares-Ramos, R. Sarrias-Mena, P. García-Triviño, L.M. Fernández-Ramírez, "Large-Scale Grid Connected Quasi-Z-Source Inverter-Based PV Power Plant", 2020 IEEE International Conference on Environment and Electrical Engineering and 2020 IEEE Industrial and Commercial Power Systems Europe (EEEIC / I&CPS Europe), Madrid, Spain, 2020, pp. 1-6.

[25] O. Husev, D. Vinnikov, C. Roncero-Clemente, A. Chub, E. Romero-Cadaval, "Single-Phase String Solar qZS-based Inverter: Example of Multi-Objective Optimization Design", IEEE Transactions on Industry Applications.